Journal of
Ceramic Science
and Technology

J. Ceram. Sci. Tech., 02 [02] 119-124 (2011)
DOI: 10.4416/JCST2010-00046
available online at: http://www.ceramic-science.com

Effect of Heat Treatment on Grain Growth of Nanocrystalline Hydroxyapatite Powder

I. Mobasherpour*, E. Salahi

Materials and Energy Research Center, Ceramics Department, P.O. Box 31787-316, Karaj, Iran
received December 8, 2010; received in revised form February 23, 2011; accepted March 4, 2011

Abstract

Nanocrystalline hydroxyapatite powder was synthesized with the solution-precipitation method followed by heat treatment in order to evolve phases, which were studied with XRD and TEM techniques. The crystallites sizes were estimated with the Scherrer method and results confirmed with TEM micrographs. The experimental observations showed that nanocrystalline hydroxyapatite can be successfully prepared from raw materials with the precipitation technique. Compared to other techniques, the precipitation technique is a competitive method for nanocrystalline hydroxyapatite synthesis. Moreover, a growth kinetic investigation was performed on the nanocrystalline growth process during heat treatment. Results have shown that grain sizes increase exponentially with temperature and the growth rate constants increase with time. The average activation energy of hydroxyapatite grain growth obtained 30.33 – 77.78 KJ/mol with this method.

Keywords: Hydroxyapatite, nanostructures, crystal growth, electron microscopy, X-ray diffraction

I. Introduction

Over the past several decades, hydroxyapatite (HAp: $Ca_{10}(PO_4)_6(OH)_2$) has been the focus of interest as a substitute material for damaged human teeth and/or bones owing to its excellent biocompatibility, bioactivity, osseous conductivity, and non-toxicity [1,2,4]. In addition, HAp has a similar crystallographic and chemical composition to calcified tissues of vertebrates. Moreover, apatite calcium phosphates are used in the pharmaceutical industry as direct compression excipients [3]. Several studies have discussed various powder processing techniques with the aim of achieving the most effective synthesis method to prepare HAp with well-defined particle morphology [5-8].

Solid state reaction and wet chemical routes are two main methods of preparing HAp powders. Depending upon the preparation method, materials with different morphology, stoichiometry (Ca/P atomic ratio) and crystallinity can be obtained. Solid state reactions usually give rise to a stoichiometric and well-crystallized product at the expense of relatively high processing temperatures and long heat-treatment period. The wet method can be divided into three categories: solution-precipitation method, hydrothermal technique, and finally hydrolysis of other calcium phosphates [8,9]. In the solution-precipitation method, nanosize crystals in the shapes of platelets, needles, rods, or equiaxed particles are obtained. The crystallinity and Ca/P atomic ratio of these products depend strongly upon the preparation conditions and are in many cases far from well-crystallized stoichiometric hydroxyapatite. The hydrothermal technique usually results in HAp materials with a high degree of crystallization, a Ca/P molar ratio close to the stoichiometric value, and a crystallite size in the range of several nanometers to millimeters.

Properties of HAp bioceramic may be significantly improved by controlling important parameters of powder precursors such as particle size, shape, particle size distribution, and heat treatment [10]. HAp nanocrystalline powders provide large surface areas [11], which improves sinterability and densification of the corresponding ceramics [12]. Bulk ceramics with ~ 98 % theoretical densities have been obtained by sintering compacted nanosized HAp at 1000 °C. Moreover, nanometer-sized HAp is also expected to exhibit better bioactivity than coarser HAp [13,14]. HAp ceramics with nanosized grains clearly represent a unique and promising class of orthopedic/dental implants with enhanced osseous integration properties [14,15].

Recently, the use of solution-precipitation processes for synthesis of HAp has become an important research objective [16]. In this study, the effect of heat-treatment on nano-crystallization, phase transformation, and grain growth of hydroxyapatite particles was investigated. Powder characterizations including phase composition, morphology and distribution of grain size were performed. Moreover, a simple discussion on the grain size growth rate and its activation energy is presented based on classical and new grain growth approaches.

II. Material and Methods

Hydroxyapatite powders were prepared with the solution-precipitation method using $Ca(NO_3)_2{\cdot}4H_2O$ (Analar No. 10305) and $(NH_4)_2HPO_4$ (Merck No. 1205) as starting materials and ammonia solution as an agent for pH adjustment. 250 ml of 0.29M $(NH_4)_2HPO_4$

* Corresponding author: Iman.Mobasherpour@gmail.com

solution was slowly added dropwise to the 350 ml of 0.24M $Ca(NO_3)_2{\cdot}4H_2O$ solution while this was vigorously stirred at about 25 °C. In all experiments the pH of $Ca(NO_3)_2{\cdot}4H_2O$ stock solutions was adjusted with ammonia to pH = 11. Under these conditions, a stoichiometry composition can be easily achieved based on the following reaction [17]:

$$10Ca(NO_3)_2{\cdot}4H_2O+6(NH_4)_2HPO_4+8NH_4OH \rightarrow Ca_{10}(PO_4)_6(OH)_2+20NH_4NO_3+46H_2O$$

Once the precipitation reaction was complete, the suspensions were then centrifuged at 3000 rpm for 60 seconds to remove the precipitates. The resulting powders were next dried in an oven at 80 °C for 1 hour and then calcined continually at 100, 450, 900 and 1200 °C in a tube furnace under controlled atmosphere. The heating rate was 10 K/min and air was used as the purging gas. Total time for heat treatment was 2 hours.

Phase transformation during heat treatment and crystallite size evolution were evaluated with X-ray diffraction using a Siemens diffractometer (30 kV and 25 mA) with CuKα radiation (λ = 1.5405Å) and the Scherrer method from the line broadening of the diffraction lines, respectively [18].

$$t=\frac{0.9\lambda}{B\cos\theta}$$

where t is the average grain size (nm), λ is the CuKα wave length (nm), B is the diffraction peak with a half maximum intensity (radian), and θ is the Bragg diffraction angle.

Transmission electron microscopy (TEM: FEG Philips CM 200) was also used for characterizing the size and shapes of particles. For this purpose, particles were deposited onto Cu grids, which supported a "holey" carbon film. The particles were deposited onto the support grids by deposition from a dilute suspension in acetone or ethanol. The grain shapes and sizes were characterized with diffraction (amplitude) contrast. The specific surface area was determined from N2 adsorption isotherm with the BET method using a Micromeritics ASAP 2010 surface area analyzer.

III. Results and Discussion

(1) Synthesis and heat treatment

Fig. 1 shows the X-ray diffraction (XRD) patterns of hydroxyapatite powders heat-treated at various temperatures. The XRD pattern of HAp powder heated at 100 °C shows wide peaks with low intensities without the presence of any second phase. The broadened (211), (112), (300) and (002) peaks indicate that the crystallites are very fine in nature with high atomic oscillations. All XRD patterns of powders heat-treated at different temperatures show similar profiles. However, the intensities of hydroxyapatite peaks gradually increase when the heat treatment temperature increases. This suggests further nucleation/growth of the hexagonal-dipyramidal nanocrystals. This figure also confirms that the hexagonal-dipyramidal phase, which is the stable phase of HAp at room temperature, does not transform to other phases when heated up to 1200 °C.

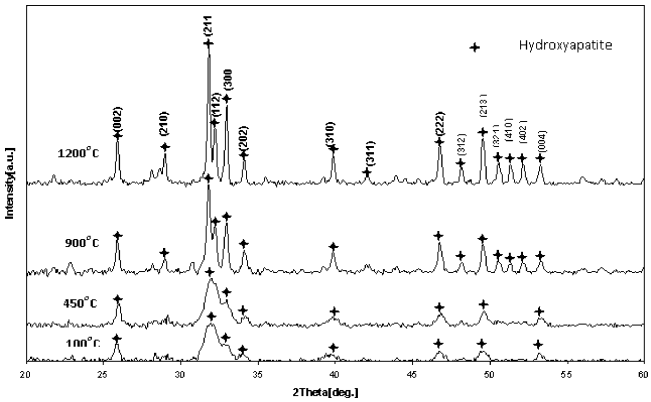

Fig. 1: XRD Patterns of heat-treated hydroxyapatite powders at different temperature.

The XRD patterns of the HAp heat-treated at 450 °C is almost similar to that treated at 100 °C. Heat treatment at 900 °C and 1200 °C results in the enhancement of peak intensities, formation of new crystallographic planes such as (112), (321), (401) and (402), peak splitting between 30° to 35°, and contraction of peak widths. This is attributed to the reduction of amorphous phase quantities, enrichment of crystallinity, and arrangement in the hydroxyapatite structure.

Table 1 lists the calculated crystallite sizes at different heat treatment temperatures based on XRD profile analysis and the Scherrer method [18-20]. In this method, the broadening contributions owing to the crystallite size are taken into account. The hydroxyapatite grain sizes gradually increased when the sample was heated from 100 °C to 1200 °C. As shown in Fig. 2, grain sizes increased exponentially with increasing temperature. Transmission electron microscopy (TEM) micrographs of the hydroxyapatite powders after heating at 100 to 1200 °C are shown in Fig. 3. TEM observations are in good agreement with XRD results. The microstructure of hydroxyapatite particles after heat treatment at 100 °C is observed to be almost like irregular circular plates, with particle size in the range of 8 - 10 nm, and the specific surface area 94.97 $m^2{\cdot}g^{-1}$. When the temperature was increased to 1200 °C, the particle size of hydroxyapatite was found to be 50 – 60 nm with roughly hexagonal shape morphology and the specific surface area measuring 2.44 $m^2{\cdot}g^{-1}$. XRD grain size was calculated with the Scherrer method and used for grain growth investigation.

Table 1: Grain size of HAp crystalline as a function of heat treatment temperature and time.

Heat treatment time [s]	Grain size [nm]	Temperature [K]
600	7.75	373
2700	8.01	723
5400	27.79	1173
7200	59.06	1473

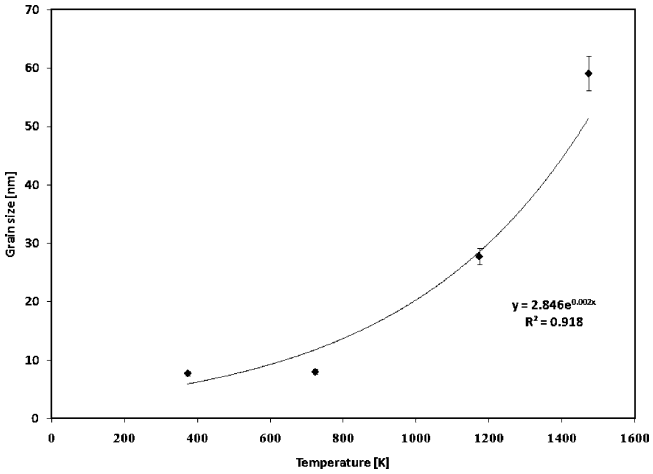

Fig. 2: Plot of growth grain sizes versus heat treatment temperature.

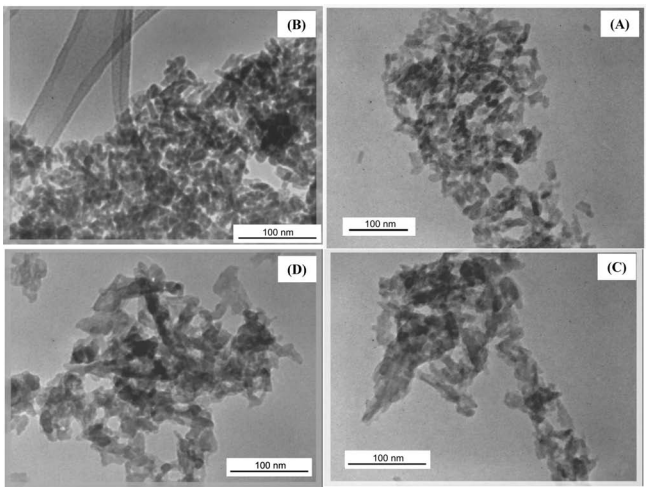

Fig. 3: TEM micrograph of hydroxyapatite powder heated at 100 °C (A), 450 °C (B) 900 °C (C) and 1200 °C (D).

(2) Grain growth investigation

As mentioned above, heating powders from 100 °C to 1200 °C is accompanied by more nucleation/growth of the nanocrystals inside the powder. Although the exact particle nucleation and growth mechanisms are not clear, nucleation occurs probably based on either hydrolytic reactions or a salting-out phenomenon. Growth could progress as a result of molecular diffusion/deposition or the aggregation of primary particles with increasing temperature.

The results in Table 1 show that during heat treatment, nanoscale grain growth has occurred. In general, grain growth occurs in polycrystalline materials to decrease the system free energy by reducing the total grain boundary energy. The earliest consideration of the kinetics of normal grain growth assumes a linear relation between the growth rate and the inverse of grain size [21]:

$$\frac{dD}{dt} = \frac{k}{D} \tag{1}$$

where D, t, and k are the mean grain diameter, heating time, and growth rate constant. The integration form of this equation is:

$$D^2 - D_0^2 = kt \tag{2}$$

And

$$k = k_0 \exp\left(-\frac{Q}{RT}\right) \tag{3}$$

where R, Q, T, and k_0 are the universal gas constant, activation energy, absolute temperature and a constant.

Here the equations (2) And (3) are used for a simple investigation of growth rate and activation energy of HAp crystallites. Approximately, a single growth process can be separated as several domains where k is constant for each domain [22]:

$$\begin{aligned}\int_{D_0}^{D_n} DdD &= \int_{D_0}^{D_1} DdD + \ldots + \int_{D_{n-1}}^{D_n} DdD \\ &= \int_{t_0}^{t_1} k_1 dt + \ldots + \int_{t_{n-1}}^{t_n} k_n dt\end{aligned} \tag{4}$$

or

$$D^2 - D_0^2 = \left\{ \begin{array}{cc} k_1 t & t \le t_1 \\ \ldots & \ldots \\ k_1 t + \ldots + k_n (t_n - t_{n-1}) & t_n > t > t_{n-1} \end{array} \right\} \tag{5}$$

k_1, k_2, ..., k_n are the growth rate constants in each domain. k_1, k_2 and k_3 values for $n = 3$ were calculated in the this study. The results are presented in Table 2 and Fig. 4. As shown, growth rate constants increase with time: $k_1 < k_2 < k_3$. The activation energy can be obtained from equation (3) as the slope of a plot of (ln k) against (1/T). This plot is shown in Fig. 5 for the minor and major temperature of every domain. The average activation energies obtained are 30.33 and 77.78 kJ/mol for the lower and higher temperatures, respectively.

Table 2: Constant growth rate in each domain.

Time range [s]	Rate constant [nm²/s]
600-2700	0.002
2700-5400	0.2623
5400-7200	1.5088

It has been mentioned that for nanoscale materials, grain growth is accompanied by a reduction in diffusion rate and increase of activation energy of diffusion [23]. It is unclear what happens in the growth process of HAp during heat treatment. F. Liu and R. Kirchheim [24] introduced a new empirical relationship using the Gibbs adsorption equation and McLean's grain boundary segregation model. This approach states that in systems with high segregation energy, decreasing grain boundary energy to zero is possible. In addition, the decrease of activation energy can be described with this equation. The grain size is proportional to the inverse exponential part of temperature within their relation:

$$D = \frac{A}{B - \exp\left(-\frac{C}{T}\right)} \tag{6}$$

where A, B, C, are const coefficients and T is temperature.

Therefore this relationship can present a better fitting for the HAp growth profile. It is well known that at high temperature (about 1673 K) the H and O atoms leave the HAp crystalline lattice, giving rise to the formation of tricalcium

phosphate, TCP. According to F. Liu and R. Kirchheim, the mobility of H and O atoms may increase at high temperature, which causes the crystallites to overcome the energy barrier at the grain boundary. This can be described as a "semi-segregation" phenomenon during heat treatment and explains corresponding changes in rate constant and activation energy at high temperatures. It should be noted that the constants in the F. Liu and R. Kirchheim relation are not known for HAp.

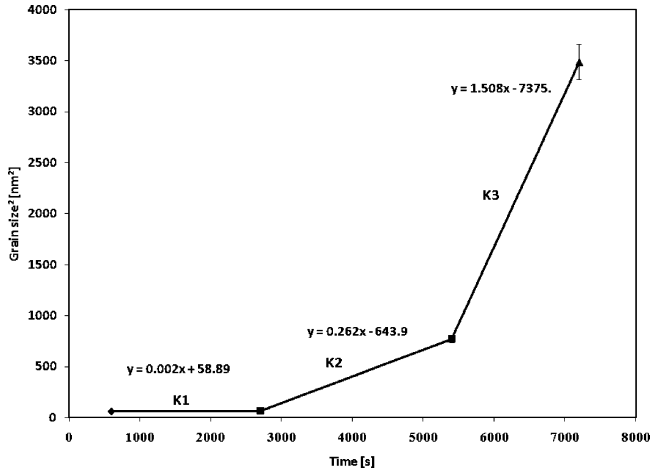

Fig. 4: Growth profile of HAp for n=3 in equation (5).

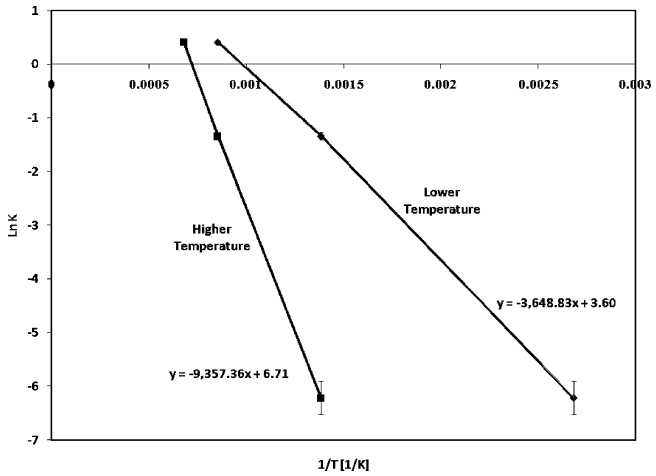

Fig. 5: Arrhenius plot of logarithm of the rate constants versus reciprocal heat treatment temperature.

IV. Conclusions

Hydroxyapatite powder with nanoparticles was successfully prepared with the solution-precipitation technique from $Ca(NO_3)_2{\cdot}4H_2O$ and $(NH_4)_2HPO_4$ solutions as starting materials. Heat treatment was performed on hydroxyapatite samples at different temperatures. The hydroxyapatite grain sizes gradually increased when the sample was heated from 100 °C to 1200 °C. According to observed growth investigation, growth rate constants increased with increasing time range. Average activation energy obtained was in the range of 30.33-77.78 KJ/mol. Considering F. Liu and R. Kirchheim's proposed new relationship, the mobility of H and O atoms may increase at higher temperatures leading to semi-segregation and may also explain the behaviors of growth rate constant and activation energy.

Acknowledgments

This work was supported by the Materials and Energy Research Center. The authors would also like to thank Dr. B. Jadedeyan for her help in improving the English of this paper.

References

1 Suchanek, W., Yoshimura, M.: Processing and properties of hydroxyapatite-based biomaterials for use as hard tissue replacement implants, *J. Mater. Res.*, **13**, [1], (1998).

2 Hench, L.L.: Bioceramics: from concept to clinic, *J. Am. Ceram. Soc.*, **74**, 1487, (1991).

3 Pontier, C., Viana, M., Champion, E., Chulia, D.: Apatitic calcium phosphates used in compression: rationalization of the end-use properties, *Powder Technology,* **130**, 436, (2003).

4 He, Z., Ma, J., Wang, C.: Constitutive modeling of the densification and the grain growth of hydroxyapatite ceramics, *Biomaterials*, **26**, 1613, (2005).

5 Ramesh, S., Tan, C.Y., Bhaduri, S.B., Teng, W.D.: Rapid densification of nanocrystalline hydroxyapatite for biomedical applications, *Ceram. Int.*, **33**, 1363, (2007).

6 Kokubo, T., Kim, H.M., Kawashita, M.: Novel bioactive materials with different mechanical properties, *Biomaterials*, **24**, 2161, (2003).

7 Gibson, I.R., Ke, S., Best, S.M., Bonfield, W.: Effect of powder characteristics on the sinterability of hydroxyapatite powders, *J.Mater.Sci.Mater.M.*, **12**, 163, (2001).

8 Aoki, H.: Science and Medical Applications of Hydroxyapatite, JAAS Tokyo, (1991).

9 LeGeros, R.Z.: Calcium Phosphate in Oral Biology and Medicine, Karger AG, (1991).

10 Best, S., Bonfield, W.: Processing behaviour of hydroxyapatite powders with contrasting morphology, *J. Mater. Sci.: Mater. M.*, **5**, 516, (1994).

11 Legeros, R.Z.: Biodegradation and bioresorption of calcium phosphate ceramics, *Clin. Mater*, **14**, 65, (1993).

12 Yeong, K.C.B., Wang, J., Ng, S.C.: Fabricating densified hydroxyapatite ceramics from a precipitated precursor, *Mater. Lett.*, **38**, 208, (1999).

13 Stupp, S.I., Ciegler, G.W.: Organoapatites: Materials for artificial bone. I. Synthesis and microstructure, *J. Biomed. Mater. Res.*, **26**, 169, (1992).

14 Webster, T.J., Ergun, C., Doremus, R.H., Siegel, R.W., Bizios, R.: Enhanced osteoclast-like cell functions on nanophase ceramics, *Biomaterials*, **22**, 1327, (2001).

15 Webster, T.J., Siegel, R.W., Bizios, R.: Osteoblast adhesion on nanophase ceramics, *Biomaterials*, **20**, 1221, (1999).

16 Han, Y., Li, S., Wang, X., Chen, X.: Synthesis and sintering of nanocrystalline hydroxyapatite powders by citric acid sol-gel combustion method, *Mater. Res. Bull.*, **39**, 25-32, (2004).

17 Mobasherpour, I., Soulati Heshajin, M., Kazemzadeh, A., Zakeri, M.: Synthesis of nanocrystalline hydroxyapatite by using precipitation method, *J. Alloy. Compd.*, **430**, 330, (2007).

18 Cullity, B.D.: Elements of X-ray Diffraction, Second ed., Addison-Wesley Publishing, (1977).

19 Williamson, G.K., Hall, W.H.: X-ray line broadening from filed aluminium and wolfram, *Acta Metall.*, **1**, 22-31, (1953).

20 Zakeri, M., Yazdani-Rad, R., Enayati, M.H., Rahimipour, M.R.: Synthesis of nanocrystalline $MoSi_2$ by mechanical alloying, *J. Alloy. Compd.,* **403**, 258, (2005).

[21] Atkinson, H.V.: Overview no. 65: Theories of normal grain growth in pure single phase systems, *Acta Metall.*, **36**, 469, (1988).

[22] Liu, F., Kirchheim, R.: Comparison between kinetic and thermodynamic effects on grain growth, *Thin Solid Films*, **466**, 108, (2004).

[23] Höfler, H.J., Tao, R., Kim, L., Averback, R.S., Altetetter, C.J.: Mechanical properties of single-phase and nano-composite metals and ceramics, *Nanostruct. Mater.*, **6**, 901, (1995).

[24] Liu, F., Kirchheim, R.: Nano-scale grain growth inhibited by reducing grain boundary energy through solute segregation, *J. Cryst. Growth,* **264**, 385, (2004).